Machining behavior of natural fiber composites

1. **Faissal Chegdani** [*]

   - Arts et Metiers Institute of Technology, MSMP, HESAM Université, F-51006, Châlons-en-Champagne, France.

   Email: faissal.chegdani@ensam.eu

2. **Mohamed El Mansori**

   - Arts et Metiers Institute of Technology, MSMP, HESAM Université, F-51006, Châlons-en-Champagne, France
   - Texas A&M Engineering Experiment Station, College Station, TX 77843, USA

   Email: mohamed.elmansori@ensam.eu

ABSTRACT: (50-100 words)

The machinability of thermoplastic natural fiber composites is investigated in this paper. An exploratory study is performed to investigate the effect of natural fiber type, fiber reinforcement structure, tool geometry, and process parameters on the cutting behavior of natural fibers under the usual machining processes. Results show how the cutting behavior if natural fiber is significantly sensitive to the variation of the different studied parameters. The paper is concluded by technical recommendations to improve the machinability of natural fiber composites.

KEYWORDS: (10-15 keywords)

Natural fibers; Thermoplastic polymers; Machining; Orthogonal cutting; Milling; Drilling; Mechanical properties; Cutting edge radius; Helix angle; Rake angle; Fiber orientation; Cutting speed; Cutting feed; Cutting depth; Cutting temperature.

[*] Corresponding author

1. Introduction

Natural fiber composites (NFC) are in increased demand from automotive and aerospace industries (Akampumuza et al., 2017; Pandey et al., 2010; Shalwan and Yousif, 2013). Natural fibers can compete with synthetic glass fibers in terms of mechanical (Dittenber and GangaRao, 2012; Pickering et al., 2016), thermal and acoustic properties (Alves et al., 2010; Etaati et al., 2014; Rajeshkumar and Hariharan, 2014). Moreover, natural fibers are biodegradable and recyclable which make them eco-friendly and suitable for both circular economy and sustainable development (Ramesh et al., 2017). NFC considered here are the assembly of natural fibers and polymeric matrices. If the polymer matrix is also bio-based, the NFC can be also called a green composite.

Industrial applications require high finishing quality of NFC parts, which is difficult to achieve with the usual elaboration processes such as the thermocompression technique for long continuous fiber composites (Davim and Reis, 2005; Nassar et al., 2017). Indeed, NFC parts elaborated with thermocompression have usually a poor surface quality on the edges and should be reworked. Furthermore, some specific geometries such as holes for assembly cannot be gotten directly from the thermocompression. Therefore, machining operations are essential for this type of material in order to transform the NFC part to its final industrial application.

The microstructure of natural fibers is completely different from that of synthetic glass fibers (Baley, 2002; Morvan et al., 2003). Consequently, the thermomechanical response of NFC is not similar to that of glass fiber composites (Khan et al., 2011). The machining behavior of NFC requires hence a new investigation. For this aim, this chapter presents an exploratory study that investigates the machining behavior of NFC for different natural fibrous structures, different machining processes, and different

machining parameters. This will provide to the reader a global idea about the machinability of these eco-friendly materials.

2. Natural fiber structure: from plant stem to cellulose microfibrils

The main natural fibers used in the composite industry are bast fibers extracted from the plant stem such as flax and hemp (Yu, 2015). The use of natural bast fibers is due to their high mechanical performances shown above all in their natural role of ensuring the rigidity of the plant stem.

Natural fibers are present in the plant stem in the form of a bundle of elementary fibers as shown in Figure 1. These fiber bundles are extracted after retting of plant stem with a specific mechanical process of breaking and scutching (Sadrmanesh and Chen, 2019; Zimniewska et al., 2011). Then, the fiber bundles are hackled to separate the elementary fibers as much as possible. The resulting fibers are called technical fibers which are in form of reduced bundles of 3 to 6 elementary fibers. The elementary fiber has a cellulosic structure in form of a stacking of cellulosic cell walls (Baley, 2002). Each cell wall is itself a composite structure at nanoscale with cellulose microfibrils embedded in amorphous matrix mainly made of pectin and hemicellulose (Charlet et al., 2007).

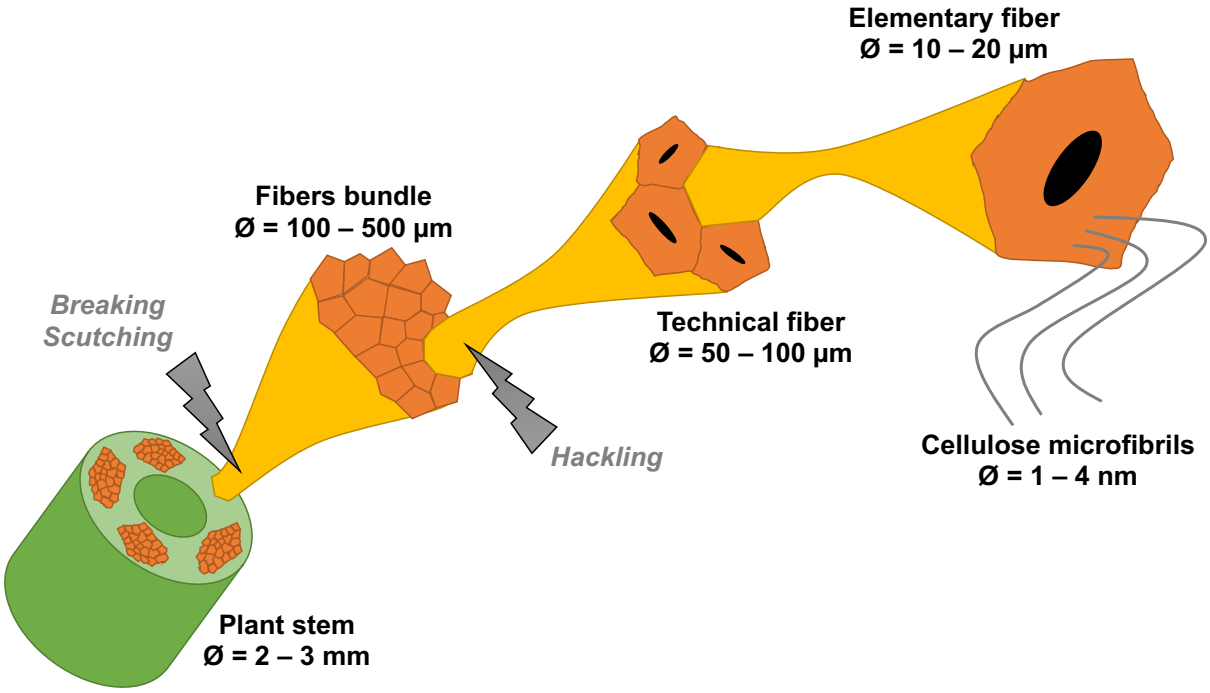

Figure 1: Schematic illustration of bast fiber structure from their plant stem to cellulose

3. Experimental methodology

3.1. Natural fibrous reinforcements

In this exploratory study, the main fibrous reinforcement structures commonly used in composites industry are investigated as shown in Figure 2:

- Random distributed short fibers:
    - Bamboo fiber composites (Bamboo FC)
    - Miscanthus fiber composites (Miscanthus FC)
    - Sisal fiber composites (Sisal FC)
- Unidirectional long fibers: Unidirectional flax fiber composites (UD flax FC)
- Bidirectional long fibers: Bidirectional flax fiber composites (BD flax FC)

Short fibers have an average length of 1 mm (Figure 2(a,b,c)). The unidirectional flax reinforcement is performed with twisted fiber yarns. The unidirectionality of flax yarns

is insured by weft synthetic fibers (Figure 2(d)). For BD flax FC, the flax fiber reinforcement is in the form of 4 ×4 plain weave of the twisted flax yarns (Figure 2(e)).

All the considered composite structures have a similar polymer matrix of polypropylene. Short fiber composites are elaborated using the thermo-injection process while the long fiber composites are manufactured with the them-compression technique. Table 1 presents the principal mechanical properties of the studied composites and their corresponding fibers.

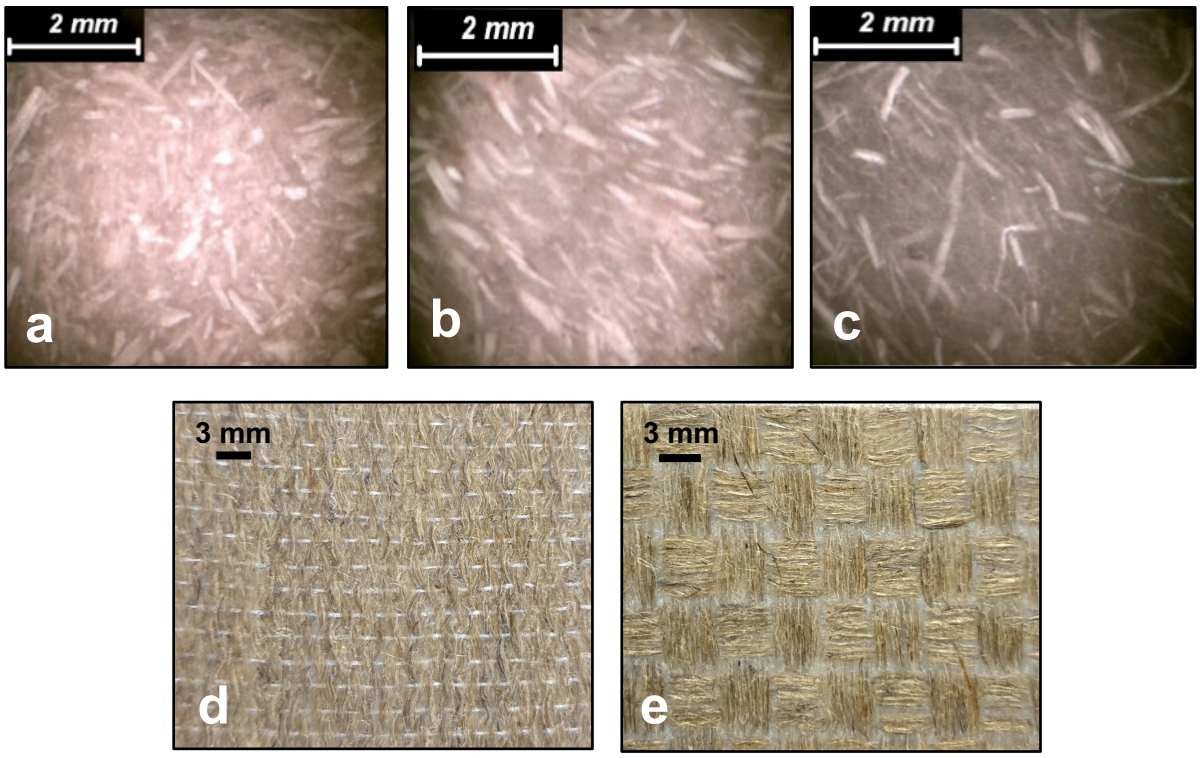

Figure 2: Photographic images of each considered NFC. (a) Bamboo FC, (b) Miscanthus FC, (c) Sisal FC, (d) UD flax FC, and (e) BD flax FC

Table 1: Mechanical properties of the considered NFC

	PP Bamboo	PP Miscanthus	PP Sisal	PP UD flax	PP BD flax
Elastic modulus (GPa)	4.1	2.7	2.2	17.6	8.1
Tensile strength (MPa)	40	30	28	109	56
Elastic modulus of fibers (GPa)	19	13.8	7.84	50	50
Tensile strength of fibers (MPa)	89.2	62	50	500	500

3.2. Machining processes

Figure 3 summarizes the machining processes investigated in this study that are the traditional techniques commonly used in composite industry such as drilling and milling. The milling process is used to rework and resize the edge of the composite parts, while the drilling process is used to create the assembly holes on the composite parts. Moreover, the fundamental process of orthogonal cutting is also used to understand the elementary cutting mechanisms of this kind of materials.

Drilling and milling were performed using a CNC machine, while the orthogonal cutting was conducted with a shaper machine. Each machining process is instrumented with a piezoelectric dynamometer to apprehend the in-situ cutting forces. In addition, the orthogonal cutting device is equipped with a fast camera to capture the in-situ chip morphology.

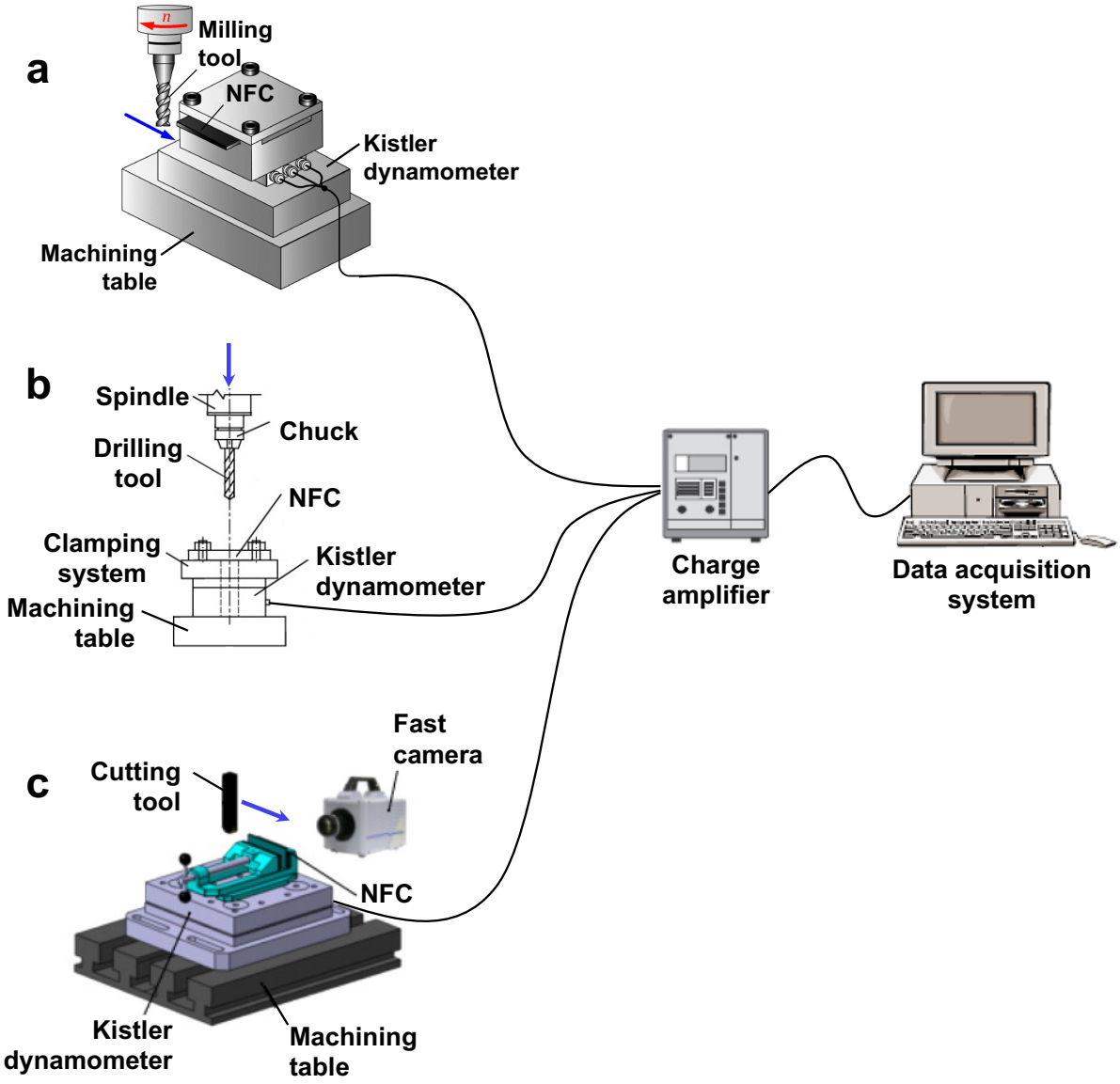

Figure 3: Schematic illustration of the experimental machining setup. (a) milling, (b) drilling, and (c) orthogonal cutting

3.3. Machining analyses

Machined surfaces are analyzed in terms of microscopic surface state and surface topography. The microscopic surface state observations are performed with a scanning electron microscope (SEM) at low vacuum mode to investigate the cutting behavior of the natural elementary fibers within the composite structure. The resulting

machined surfaces topography is quantified using a 2D stylus profilometer according to the ISO4287 standard, and 3D white light interferometer.

4. Analysis of machining behavior of natural fiber composites

4.1. Effect of fiber type

The effect of fiber type is investigated on the NFC reinforced with short fibers of bamboo, miscanthus and sisal using the milling process (F Chegdani et al., 2015). All the machining parameters are kept constant except the feed that varies from 0.04 to 0.12 mm/tooth. The machining analysis is performed by:

- Calculating the specific cutting energy;
- Observing the machined surfaces by SEM;
- Measuring the machined surfaces topography using the 2D profilometer before and after the machining operation.

The effect of the advance will be discussed later in this chapter (section 4.4.2).

Figure 4 presents the microscopic machined surface state of each NFC with the corresponding topographic signal at the same cutting conditions. Bamboo fiber composites show the best fiber shearing without significant breaking of interfaces (Figure 4(a)). Miscanthus fiber composites have also a good fiber shearing but interfaces break is noticed, especially between the elementary fibers (Figure 4(b)). For sisal fiber composites, it can be seen a significant deformation of fibers toward the feed direction before shearing. This induced uncut fiber extremities that remain on the machining surfaces in addition to important decohesion zones due to interfaces break (Figure 4(c)).

Figure 4 shows that the corresponding topographic signal of the machined surfaces reflects the phenomena observed in the SEM images. The topographic signal of Bamboo fiber composites shows the lowest irregularities (Figure 4(d)) while that of sisal fiber composites reveals the highest irregularities (Figure 4(f)). This indicates that the shearing of natural fibers differs in function of the fiber type and can be confirmed by analyzing the specific cutting energy of the three NFC as shown in Figure 5(a). Indeed, the specific cutting energy of sisal fiber composites reveals the highest values while that of bamboo fiber composites shows the lowest. This means that the fiber shearing is the most effective in the case of bamboo and the least effective in the case of sisal. Consequently, cutting NFC with sisal fibers induces high surface roughness as shown in Figure 5(b) because of uncut fibers extremities and interfaces break. This cutting behavior of natural fibers is due to their mechanical properties, especially the fiber rigidity that controls the cutting contact stiffness. As shown in Table 1, bamboo fibers have the highest rigidity and sisal fibers express the lowest one. Therefore, for next sections, the investigations will be performed on flax fiber reinforced polypropylene composites since flax fibers have the highest elastic modulus comparing to the other natural fiber types.

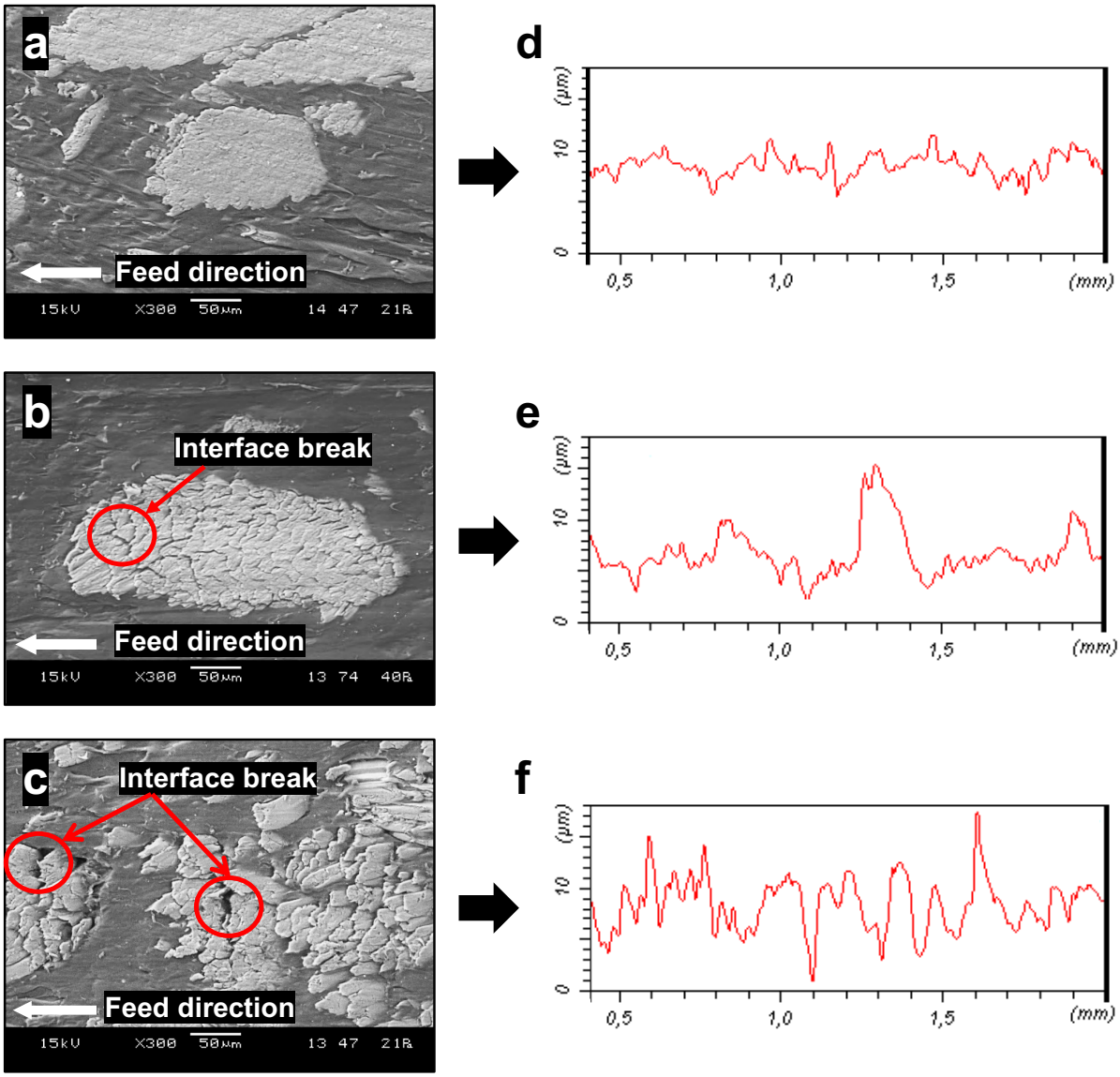

Figure 4: Typical SEM images and their corresponding topographic signals of machined surfaces for (a,d) Bamboo FC, (b,e) Miscanthus FC, and (c,f) Sisal FC

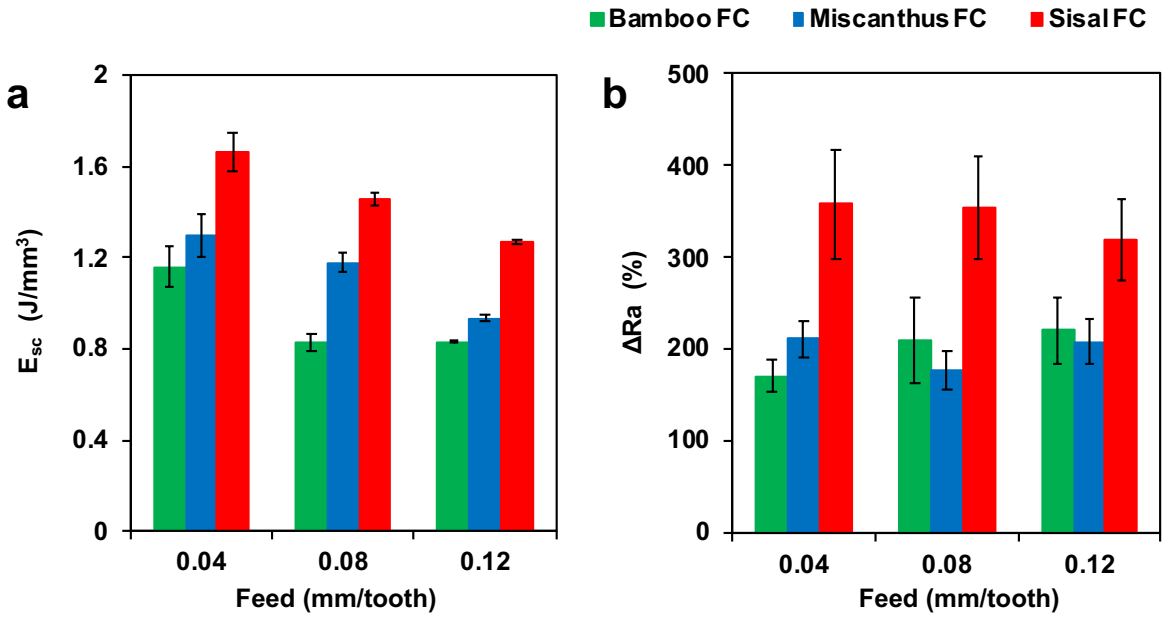

Figure 5: (a) Specific cutting energy of the short NFC. (b) Roughness gain ratio of the machined surfaces for the short NFC

4.2. Effect of fiber orientation

In this section, UF flax FC are considered. The orthogonal cutting process is used in order to isolate the fiber orientation effect. The three principal fiber orientation with respect to the cutting direction are investigated (θ = 0º, θ = 45º, and θ = 90º). Only the effect of fiber orientation is discussed in this section.

Figure 6 shows that the cutting behavior of flax fibers differs by changing their orientation relative to the cutting direction. Cutting with θ = 90º induces significant uncut fiber extremities that remain on the machined surface (Figure 6(a)). The fiber shearing is the most effective with θ = 45º where the uncut fiber extremities are not obvious on the machined surface (Figure 6(b)). For θ = 0º, the cutting behavior is random where flax fibers are either sheared, detached or torn-off (Figure 6(c)) which is related to the random cutting contact location. This random cutting behavior induces the highest surface roughness as shown in Figure 7(b). The non-effective fiber shearing in the

case of θ = 90º is noticed with the highest shearing energy as shown in Figure 7(b) while the cutting configuration with θ = 45º induces the lowest cutting energy and the lowest machined surface roughness. The poor fiber shearing when θ = 90º is due to the high transverse elasticity of natural fibers that favors the transverse deformation during the contact with the cutting tool. For θ = 45º, the shearing effectiveness is related to the fact that the fiber orientation (i.e. the highest stiffness direction) is toward the shearing plan of the cutting system.

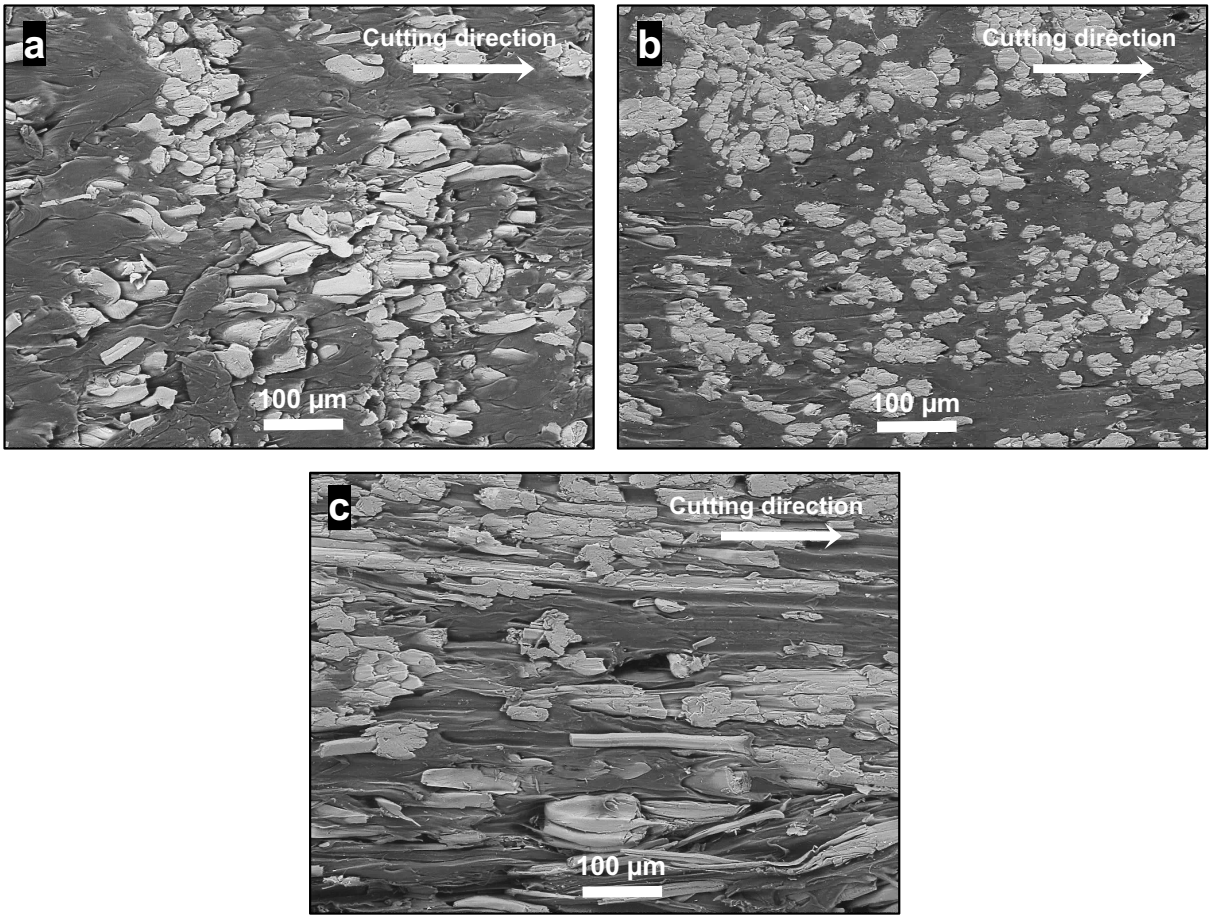

Figure 6: SEM images of the machined surfaces of UF flax FC with different fiber orientation. (a) θ = 90º, (b) θ = 45º, and (c) θ = 0º

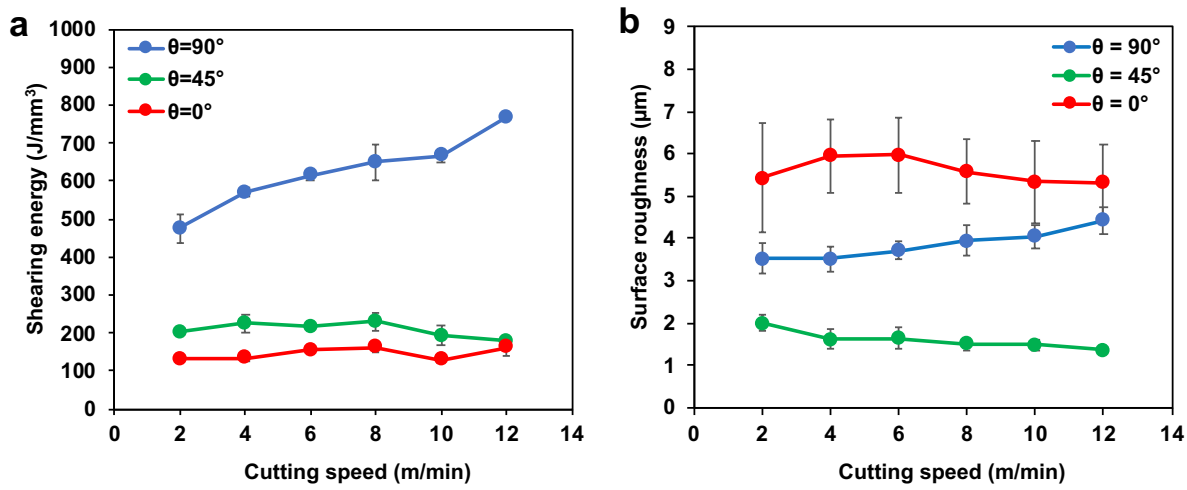

Figure 7: (a) Specific shearing energy of UD flax FC for different fiber orientations. (b) Arithmetic surface roughness of machined surfaces of UD flax FC for different fiber orientations.

4.3. Effect of tool geometry

4.3.1. Effect of cutting edge radius

In this section, milling and drilling processes are considered. For both processes, the variation of the cutting edge radius is controlled by the tool coating. Therefore, the lowest cutting edge radius is obtained with the uncoated cutting tool. Then, titanium diboride (TiB2) and diamond coatings are applied to increase the cutting edge radius. TiB2 coating is performed by monolayer physical vapor deposition (PVD) while diamond coating is achieved using multilayer chemical vapor deposition (CVD). Consequently, the two coating depositions techniques generate different coating thicknesses and lead to vary the cutting edge radius. Table 2 summarizes the tools coatings characteristics.

Table 2: Coating characteristics of drilling and milling tools

		Uncoated	TiB2 coated	Dia. coated
Milling tools	**Substrate**	carbide	carbide	carbide
	Coating thickness (µm)	-	$2^{\pm 0.7}$	$7^{\pm 1}$
	Measured cutting edge radius (µm)	$5.3^{\pm 0.6}$	$7.5^{\pm 0.5}$	$11.3^{\pm 0.7}$
Drilling tools	**Substrate**	carbide	carbide	carbide
	Coating thickness (µm)	-	$2^{\pm 0.7}$	$7^{\pm 1}$
	Measured cutting edge radius (µm)	$5.5^{\pm 0.5}$	$8^{\pm 0.5}$	$11.5^{\pm 1}$

- Effect of cutting edge radius in milling process

The investigation of cutting edge radius effect in milling process is performed on UD flax FC (Faissal Chegdani et al., 2015). The SEM images of Figure 8 reveal the high impact of the cutting edge radius on the machining behavior of NFC. Flax fibers are well sheared with the uncoated milling tool that has the sharpest cutting edge (Figure 8(a)). Increasing the cutting edge radius by about 6 µm changes completely the cutting behavior of flax fibers where a high rate of uncut fiber extremities are noticed in the machined surfaces (Figure 8(c)). This shows that the shearing effectiveness of fibers is significantly affected, and the cutting behavior of flax fibers is highly sensitive to the small variation of the cutting edge radius.

The effect of the cutting edge radius on the shearing behavior of UD flax FC is also depicted in the energetical analysis of Figure 9(a) where the highest edge radius induces the highest specific cutting energy. Consequently, the uncut fiber extremities caused by the poor fiber shearing generates the highest surface roughness as shown in Figure 9(b).

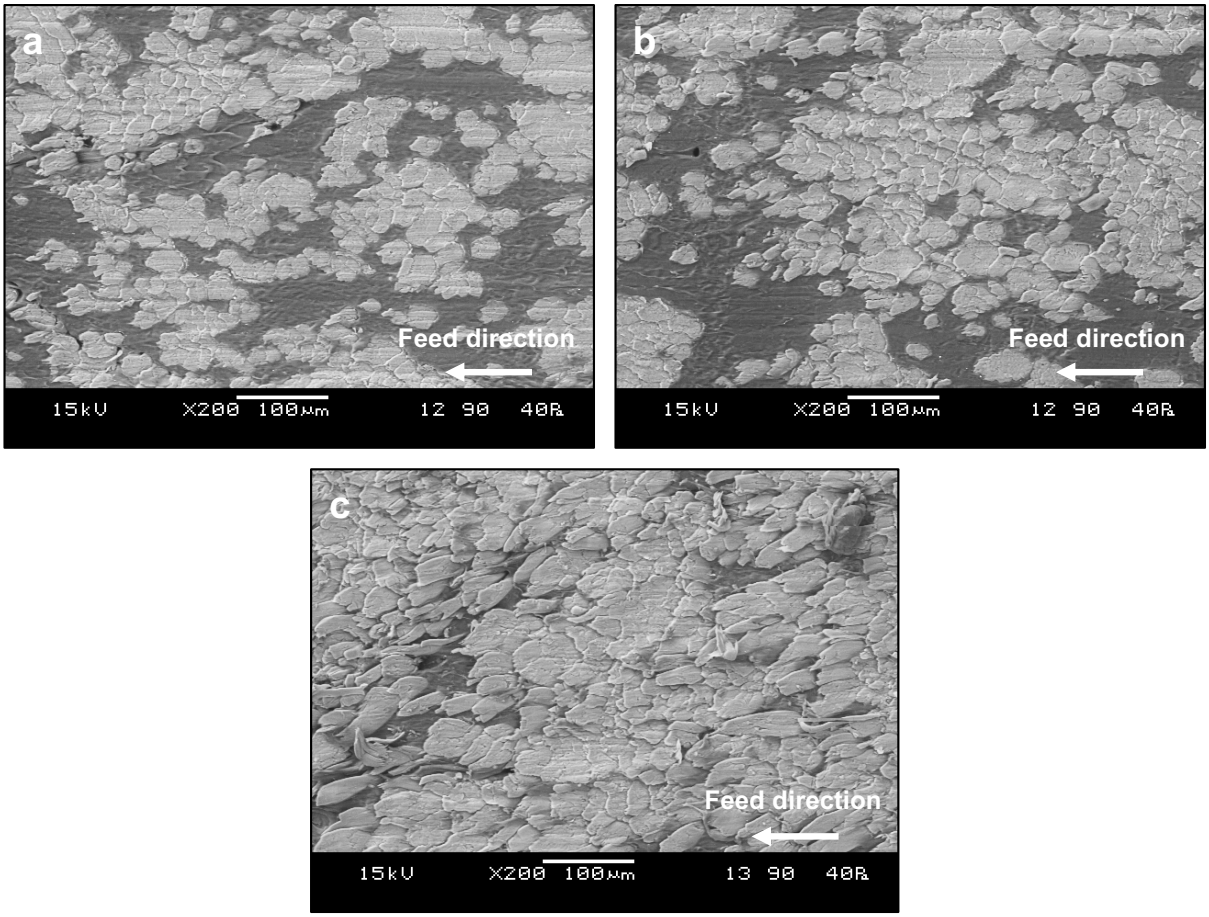

Figure 8: SEM images of the milled surfaces of UD flax FC with different values of cutting edge radii. (a) rε = 5.3 µm, (b) rε = 7.5 µm, and (c) rε = 11.3 µm

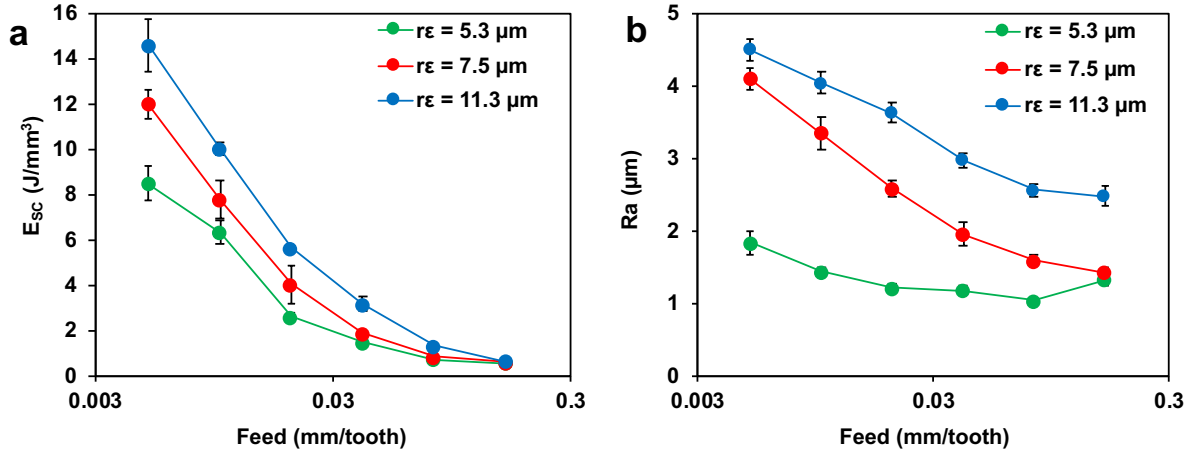

Figure 9: (a) specific cutting energy, and (b) Arithmetic surface roughness of milled surfaces for UD flax FC with different values of cutting edge radii

- Effect of cutting edge radius in drilling process

For the drilling process, the analysis of the cutting edge radius effect is performed on BD flax FC (Chegdani and El Mansori, 2018). The cutting behavior of flax fibers during the drilling operation shown in Figure 10 is similar to that of the milling process presented previously in **Erreur ! Source du renvoi introuvable.**. Indeed, drilling with the lowest cutting edge radius enhance the shearing behavior of flax fibers as shown in Figure 10(a) where the fibers cross sections are well perceptible. Flax fibers start to deform transversely when increasing the cutting edge radius from 5.5 µm to 8 µm. Uncut fiber extremities are then noticeable in the machined surface of Figure 10(b). When drilling with a cutting edge radius of 11.5 µm, the cutting behavior is completely changed from shearing to torn-off as clearly shown in Figure 10(c).

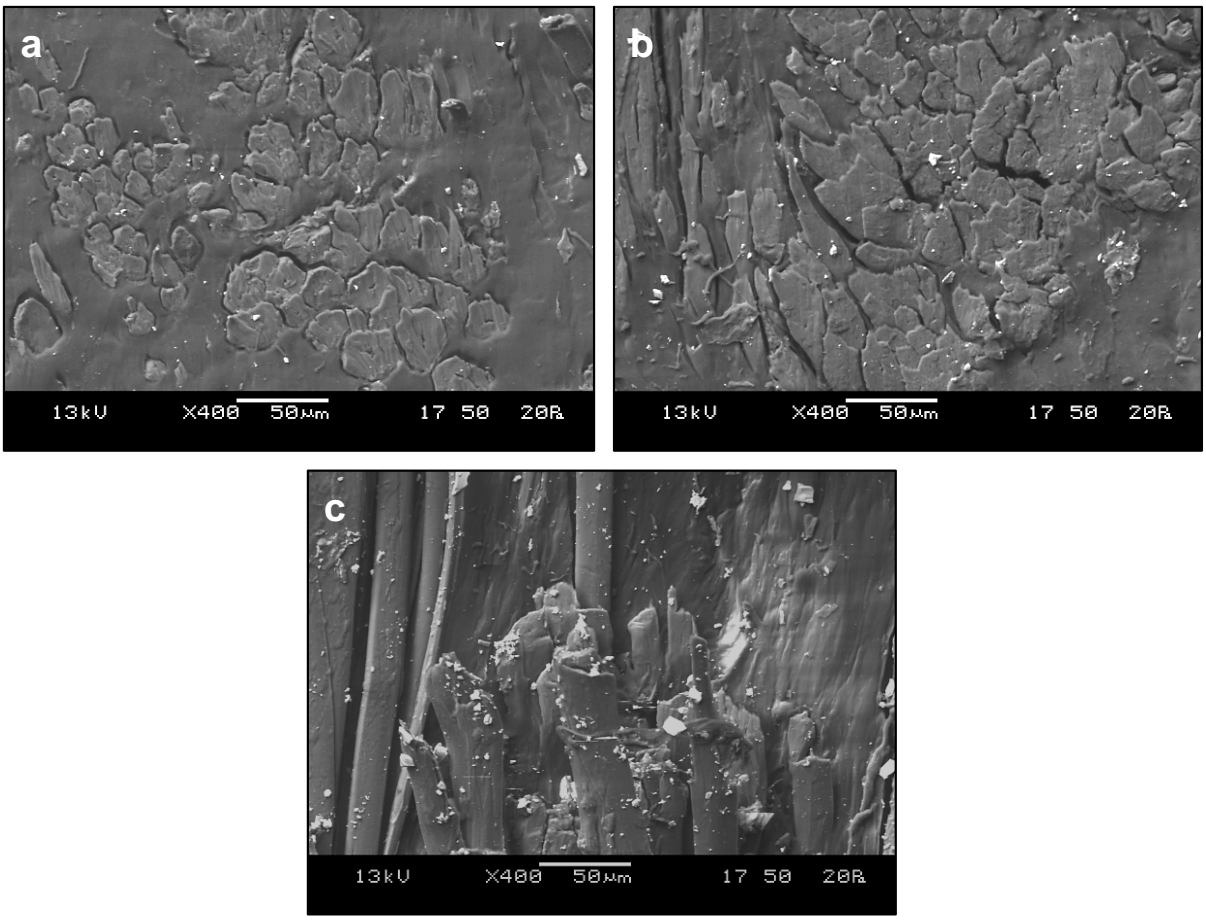

Figure 10: SEM images of the drilled surfaces of BD flax FC with different values of cutting edge radii. (a) $r\varepsilon$ = 5.5 µm, (b) $r\varepsilon$ = 8 µm, and (c) $r\varepsilon$ = 11.5 µm

The cutting behavior of flax fibers inside the composite is also exposed in the measured cutting energy as shown in Figure 11. The specific cutting energy of the drilling operation with a cutting edge radius of 11.5 µm is largely higher than the other configurations. This shows once again how small variations of the cutting edge radius can affect the cutting behavior of NFC. This is due to the cutting contact scale, specifically the contact scale between the cutting edge and the natural fibers. The diameter of elementary flax fibers is between 10 µm and 20 µm, which is in the same order of magnitude than the cutting edge radius. Therefore, when the cutting edge radius value approaches the diameter of the fiber, this latter is more likely to deform than to shear. If the cutting edge radius is greater than or equal to the fiber diameter, the fiber torn-off become the main cutting mechanism.

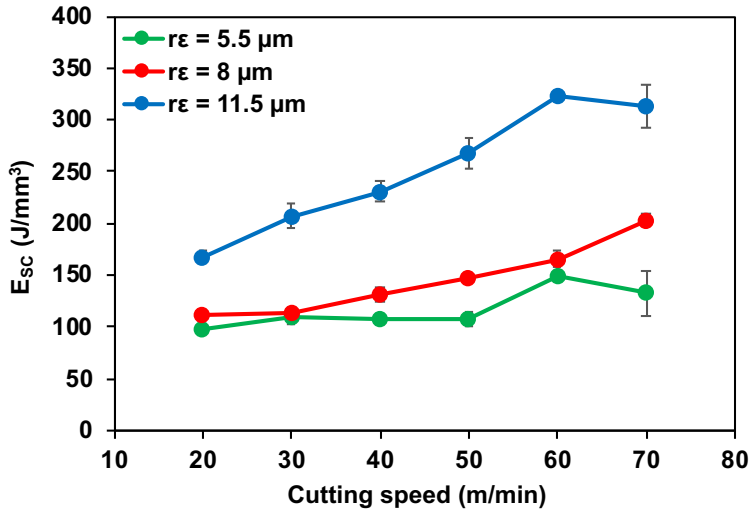

Figure 11: Specific cutting energy of drilled surfaces for BD flax FC with different values of cutting edge radii

4.3.2. Effect of helix angle

The effect of the helix angle is investigated through a milling process of BD flax FC (Chegdani et al., 2016). Three milling tools with similar geometrical parameters, except the helix angle of the cutting edges, have been considered. The helix angles values vary from H=0° to H=40°. Since the cutting edge radius increase impacts negatively

the cutting behavior of fibers (section 4.3.1), uncoated milling tool are chosen in this study.

The SEM images of Figure 12 discriminate two fiber zones. Warp fiber zones (WPZ) is the zone with flax fibers that are oriented perpendicularly to the feed direction, while weft fiber zone (WTZ) is the zone with flax fibers that are oriented toward the feed direction. As for the fiber orientation of $\theta = 0^{\circ}$ in section 4.2, the cutting behavior of flax fiber in the weft fiber zone is random and depends on the cutting contact location between the cutting edge end the fibers. However, the warp fiber zone shows an effect of the helix angle on the cutting behavior of flax fibers. Cutting with zero helix angle offers the best shearing of flax fibers as shown in Figure 12(a) where the cross section of fibers is visible on the microscopic images of the machined surfaces. The shearing effectiveness decreases when increasing the helix angle as shown in Figure 12(b) and Figure 12(c) because flax fibers on the warp fiber zone are deformed toward the feed direction and uncut fiber extremities are noticeable on the machined surfaces. This cutting behavior of flax fibers in function of the tool helix angle can be explained by the behavior of the cutting forces presented in Figure 13. Indeed, cutting with zero helix angle concentrates the machining forces in the feed direction which provides a high contact stiffness for cutting (Figure 13 (a)). When increasing the helix angle, the machining forces are reoriented from the feed direction to the tool axis direction until becoming similar for $H = 40^{\circ}$. This weakens the shearing of flax fibers and favors their deformation.

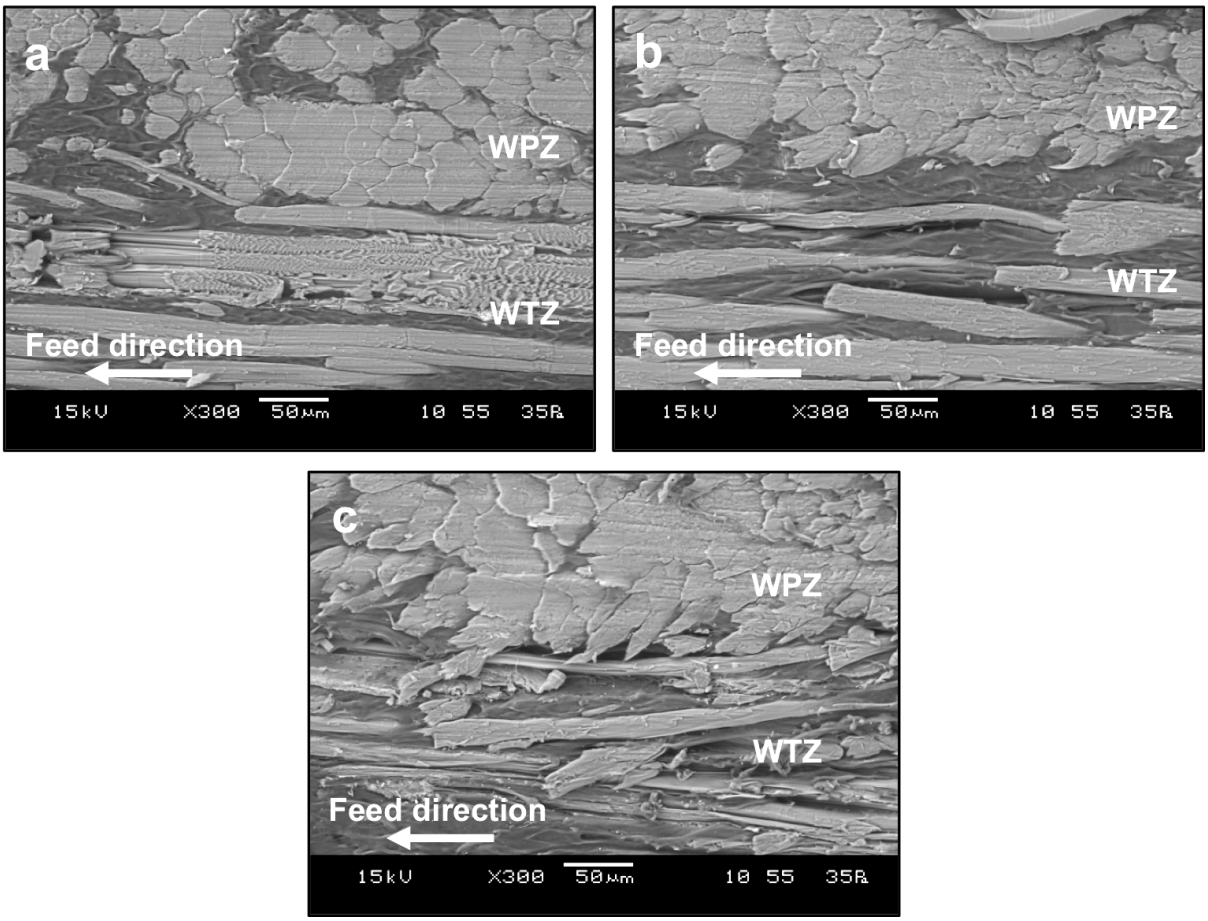

Figure 12: SEM images of the milled surfaces of BD flax FC with different values of helix angles. (a) H = 0º, (b) H = 20º, and (c) H = 40º

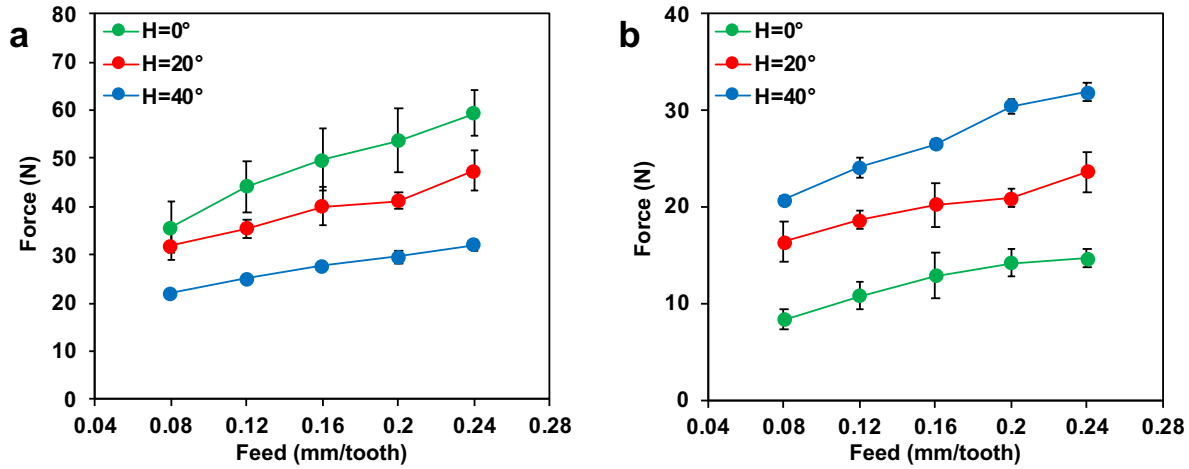

Figure 13: Machining forces of BD flax FC with different values of helix angles. (a) forces in the feed direction, and (b) forces in the tool axis direction

The effect of tool helix angle on the cutting behavior of flax fibers is revealed in the topographic analysis of the machined surfaces of BD flax FC by quantifying the arithmetic surface roughness on the warp fiber zones and the weft fiber zones

separately as shown in Figure 14. On the warp fiber zone, increasing the tool helix angle increases the surface roughness because of the uncut fiber extremities (Figure 14(a)). However, the random cutting behavior of flax fibers on the weft fiber zones induces a random trend of the surface roughness evolution with high variability in the measurements (Figure 14(b)).

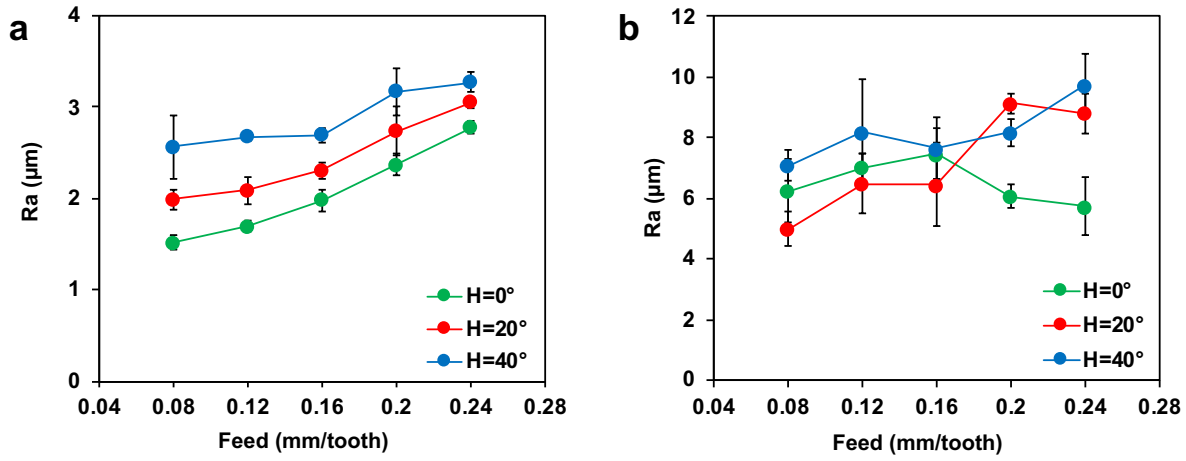

Figure 14: Arithmetic mean of the surface roughness of the machined surfaces of BD flax FC with different values of helix angles. (a) on warp fiber zones, and (b) on weft fiber zones

4.3.3. Effect of rake angle

The effect of rake angle is investigated on UD flax FC using the orthogonal cutting process (Chegdani et al., 2018b). All the cutting parameters are kept constant, except the rake angle (γ) of the cutting toll that varies from -4.5º to 5.5º.

The SEM images of Figure 15 does not show a significant difference on the microscopic surface state of the machined surfaces performed with the different values of rake angle. However, a slight enhancement of the fiber shearing is noticed on the machined surfaces achieved with positive rake angles (Figure 15(c,d)). Concretely, negative rake angles cause transverse deformation of flax fibers toward the cutting direction before shearing.

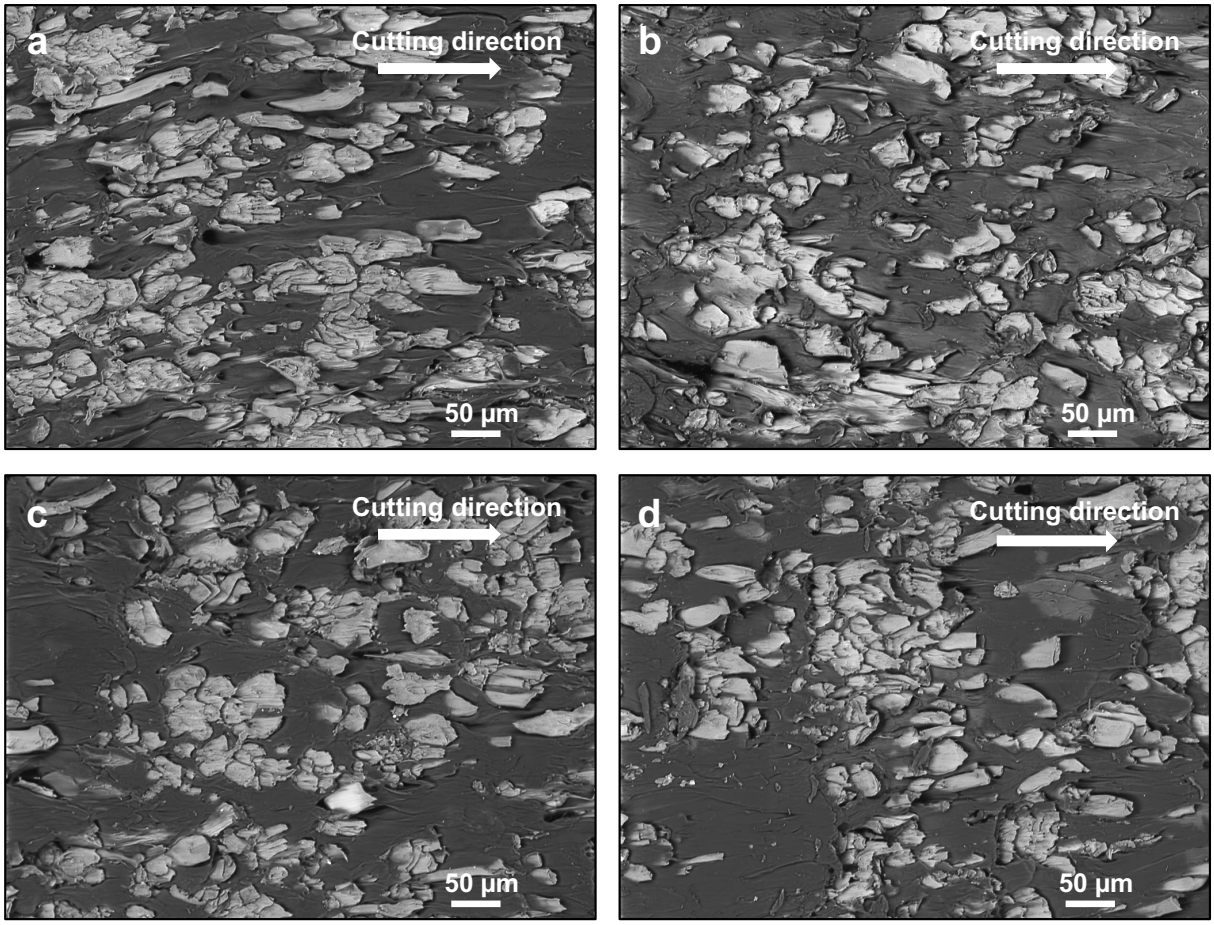

Figure 15: SEM images of the machined surfaces of UD flax FC with different values of rake angles. (a) γ = -4.5º, (b) γ = 0º, (c) γ = 3º, and (d) γ = 5.5º

On the other hand, changing the tool rake angle affects the chip morphology in terms of chip curling. As shown in Figure 16, cutting with negative rake angle avoid the curling of the chip during its formation (Figure 16(a)). Increasing the rake angle from negative to positive values favors the chip curling (Figure 16(c)). Even if the fast-cam images of Figure 16 were taken at the same cutting time, it can be seen that the chip length of negative rake angle is the smallest and increases with rake angle increase. Indeed, negative rake angle compress the material toward the shear zone which cause a plastic deformation of the removed chip by compression. Consequently, the chip thickness increases, and the chip length decreases.

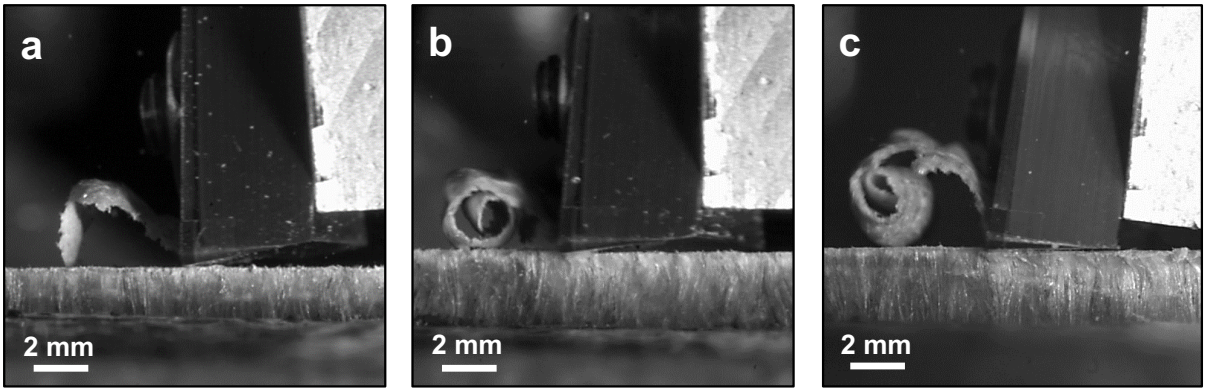

Figure 16: Fast-cam images on the same cutting time of the chip formation generated with different values of rake angles. (a) γ = -4.5º, (b) γ = 0º, and (d) γ = 5.5º

The tool rake angle affects significantly the cutting force. As sown in Figure 17(a), increasing the rake angle from -4.5º to 5.5º generates a 76% increase in cutting force. This reveals the importance of considering the rake angle effect for the design of the machining operations of NFC in order to prevent the tool wear.

The effect of rake angle presented on the SEM images of Figure 15 is reproduced with the topographic analysis of the machined surfaces as shown in Figure 17(b). Indeed, the mean arithmetic surface roughness of the machined surfaces decreases slightly by increasing the rake angle from -4.5º to 5.5º.

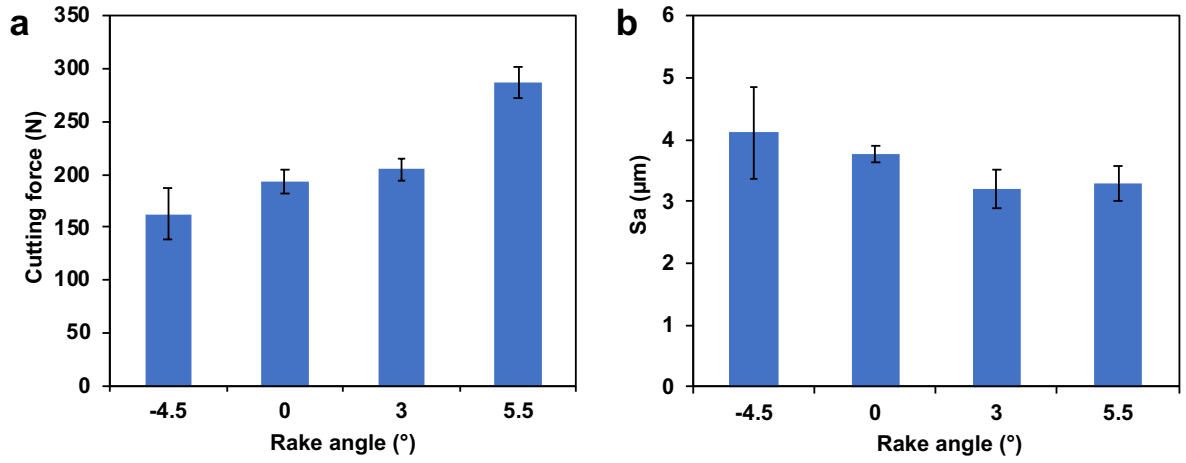

Figure 17: (a) Cutting force of UD flax FC with different values of tool rake angles. (b) 3D arithmetic mean surface roughness of the machined surfaces of UD flax FC with different values of tool rake angles

4.4. Effect of process parameters

4.4.1. Effect of cutting speed

The effect of cutting speed was presented previously in Figure 7 for the orthogonal cutting process of UD flax FC. Small cutting speed values were used in this investigation to avoid heat generation. Figure 7(a) shows that the cutting speed impacts the machining of NFC with fibers oriented perpendicularly to the cutting direction. In this cutting configuration, increasing the cutting speed increases the shearing energy of the cutting process. However, the effect of the cutting speed the surface topography is not significant (Figure 7(b)). The same observation is noticed in the case of the drilling process as shown in Figure 11 where increasing the cutting speed increases the cutting energy.

The effect of cutting speed is investigated in depth using orthogonal cutting of UD flax FC and realistic cutting speed values from 12 m/min to 80 m/min (Chegdani et al., 2018a). the SEM images of Figure 18 shown the important role of the cutting speed for the enhancement of the shearing effectiveness of flax fibers. Indeed, increasing the cutting speed from 12 m/min to 80 m/min reduces significantly the uncut fiber extremities and the decohesion zones caused by the damage of the interfaces.

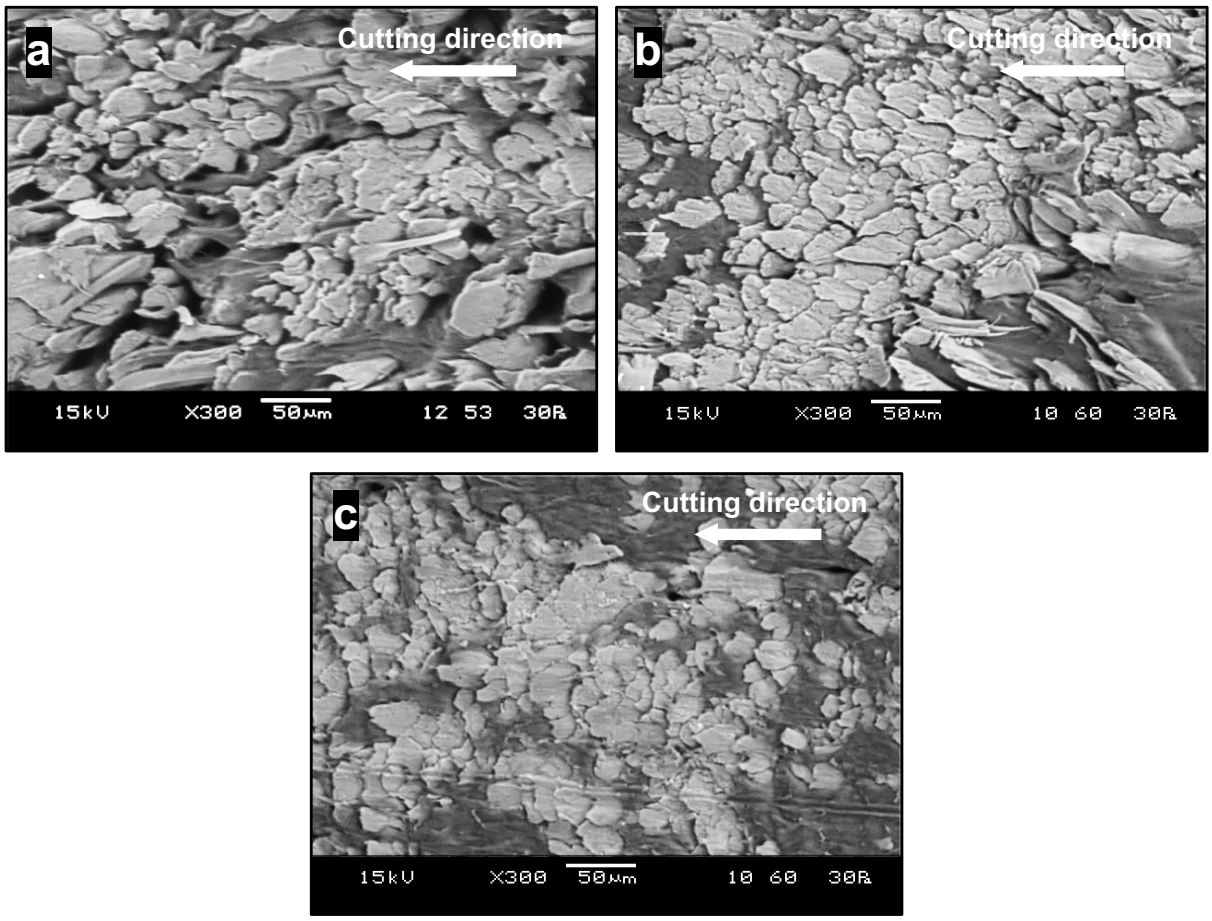

Figure 18: SEM images of the machined surfaces of UD flax FC with different values of cutting speed. (a) Vc = 12 m/min, (b) Vc = 32 m/min, and (c) Vc = 50 m/min

Regarding the machining forces, it can be seen from Figure 19 that the effect of cutting speed is similar to that observed in Figure 7 and Figure 11 where increasing the cutting speed increases the machining forces. The increase of the machining forces contributes then to the enhancement of the fiber shearing and the reduction of interface damages as shown in Figure 18. It is important to notice that the effect of cutting speed on the machined surface state is activated at high speed values as shown in Figure 7(b) where the effect of cutting speed is insignificant for speed values range from 2 m/min to 12 m/min.

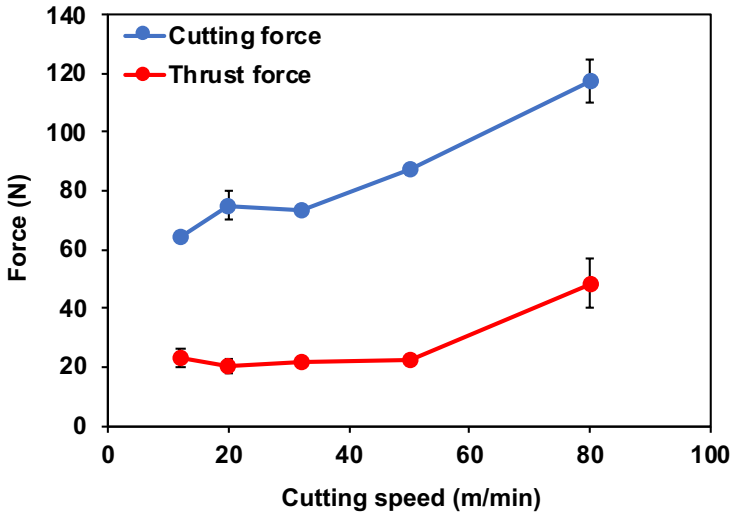

Figure 19: Machining forces of the orthogonal cutting process of UD flax FC with different values of cutting speed

4.4.2. Effect of cutting feed

The effect of cutting feed has been investigated for short fiber composites and long fiber composites using the milling process. In the case of short fiber composites (Figure 5), increasing the feed from 0.04 mm/tooth to 0.12 mm/tooth decreases the specific cutting energy which leads to a decrease of the surface roughness of the machined surfaces.

In the study of the milling process of UD flax FC (Faissal Chegdani et al., 2015), the effect of the cutting feed has been investigated deeply by exploring a large range of feed values from 0.005 mm/tooth to 0.16 mm/tooth as shown in Figure 9. The specific cutting energy of the milling process shows a significant decrease when increasing the cutting feed (Figure 9(a)). This feed increase contributes also the decrease of the machined surface roughness (Figure 9(b)).

For more understanding of the cutting feed effect, Figure 20 shows the cutting behavior of flax fibers during the milling process of UD flax FC in function of the cutting feed. It is evident that increasing the feed enhance the fiber shearing and reduces significantly the uncut fiber extremities that remain on the machined surface. As well known in the

machining fundamentals, the chip thickness is proportional to the cutting feed in the case of milling process. The chip thickness has to reach a minimum critical value to be in the favorable cutting conditions. Below this critical value, the cutting system is in the unfavorable cutting conditions that favor sliding and plastic deformation.

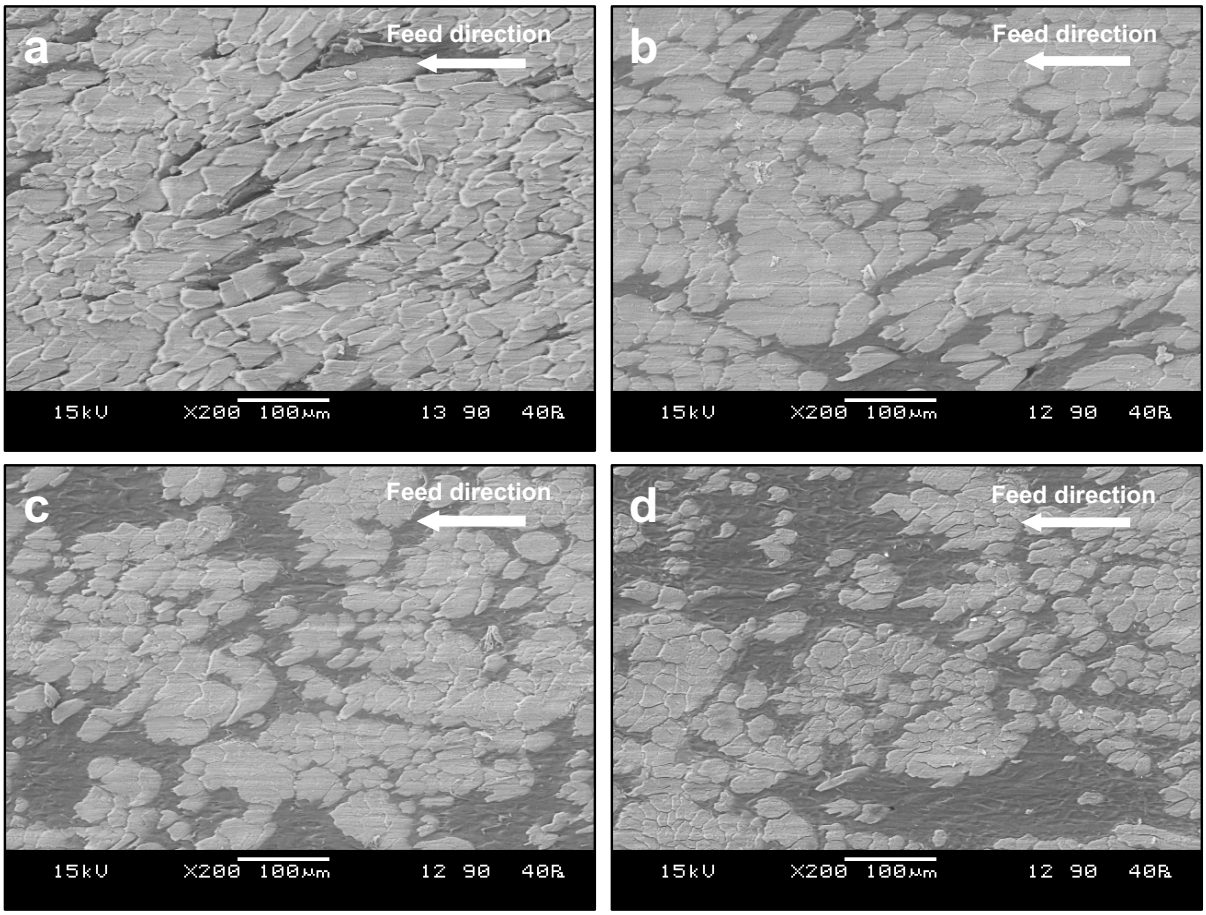

Figure 20: SEM images of milled surfaces of UD falx FC performed with different values of cutting feed. (a) f_z = 0.005 mm/tooth, (b) f_z = 0.02 mm/tooth, (c) f_z = 0.04 mm/tooth, and (d) f_z = 0.08 mm/tooth

4.4.3. Effect of cutting depth

The effect of the cutting depth is investigated in the same study of the cutting speed presented in section 4.4.1 where orthogonal cutting process is applied to UD flax FC (Chegdani et al., 2018a). The cutting depth is varied from 100 µm to 500 µm.

The fast-cam images of Figure 21 show that the chip is curled and remains continuous all over the studied range of cutting depth. This finding was also noticed all over the studied range of cutting speed of the same investigation. Moreover, the removes chip

remains also continuous when varying the fiber orientation as shown in the fac-cam images of Figure 16. The continuity of the removed chip, regardless of the machining parameters, is principally due to the ductile behavior of both flax fibers and polypropylene matrix. The high transverse elasticity of flax fibers gives them the ability to deform easily and flow the deformation motion of the cutting without brittle fractures.

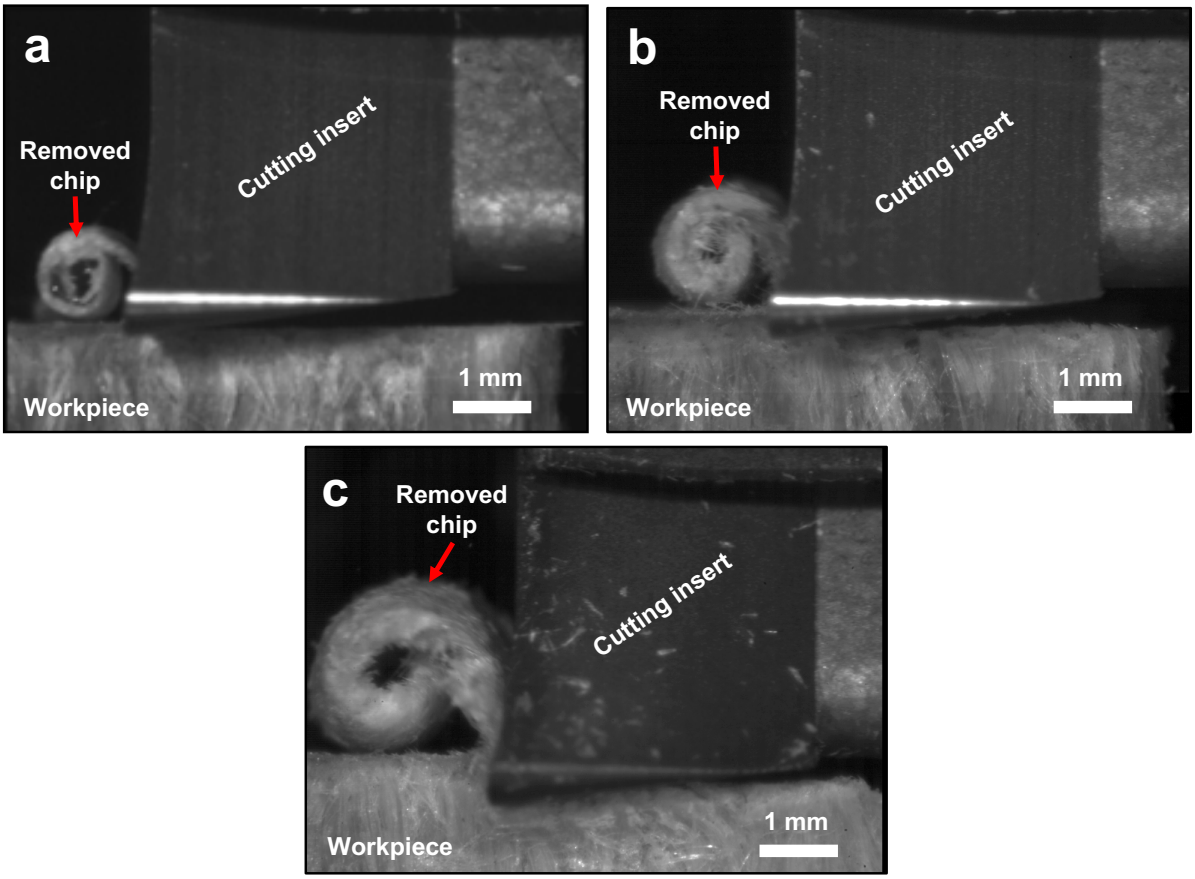

Figure 21: Fast-cam images of the chip formation generated with different values of cutting depth. (a) a_p = 100 µm, (b) a_p = 300 µm, and (d) a_p = 500 µm

SEM observation of Figure 22 reveal that increasing the cutting depth deteriorates the microscopic state of the machined surfaces. At low cutting depth (a_p = 100 µm), flax fibers show the best shearing of flax fibers with insignificant interface damages (Figure 22(a)). However, the increase of the cutting depth from 100 µm to 500 µm intensifies the transverse deformation of flax fibers in addition to decohesion zones caused by the broken interfaces (Figure 22(c)). This cutting behavior is depicted in the machining

forces presented in Figure 23 where a drastic increase of the cutting forces is noticed when varying the cutting depth from 100 µm to 500 µm. The thrust forces show a slight increase in function of the cutting depth.

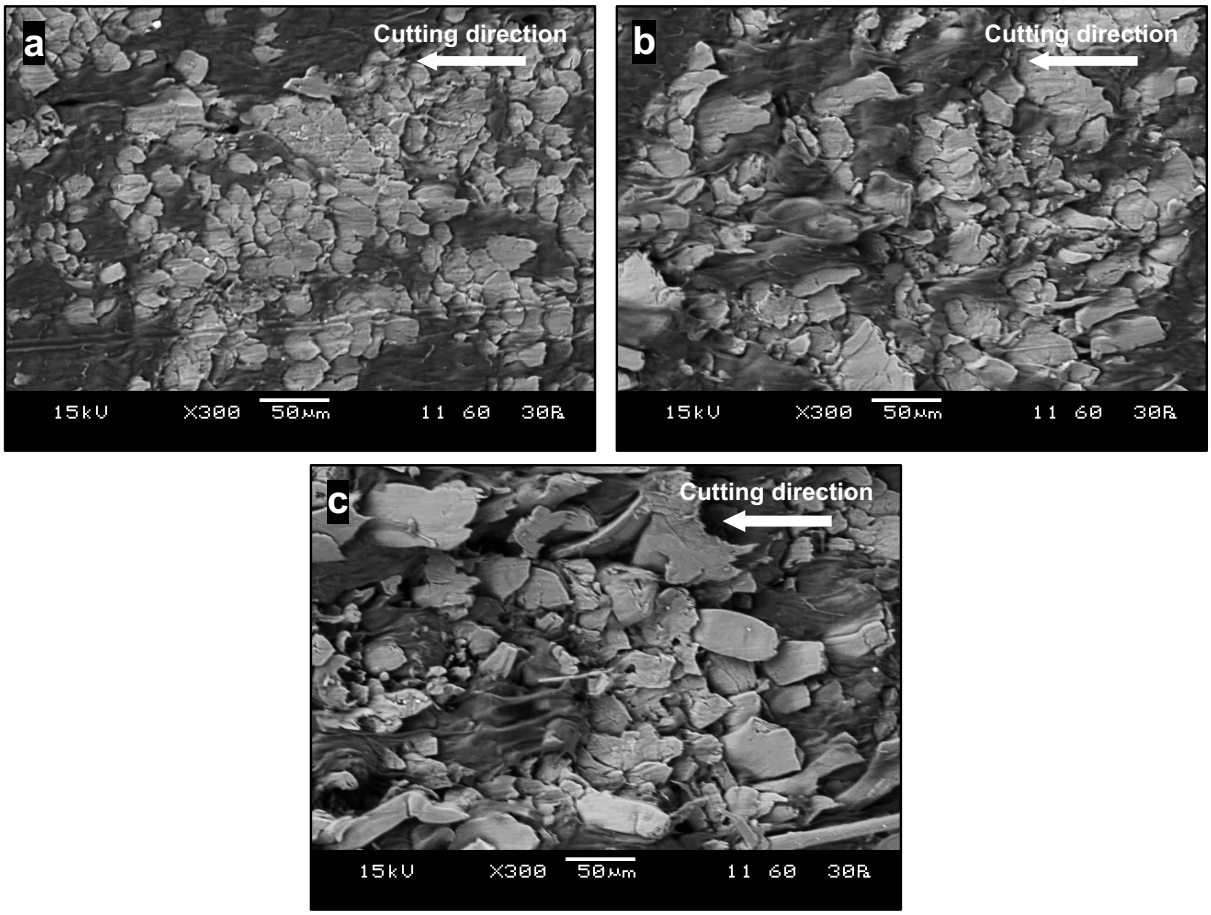

Figure 22: SEM images of the machined surfaces of UD flax FC with different values of cutting depth. (a) a_p = 100 µm, (b) a_p = 300 µm, and (c) a_p = 500 µm

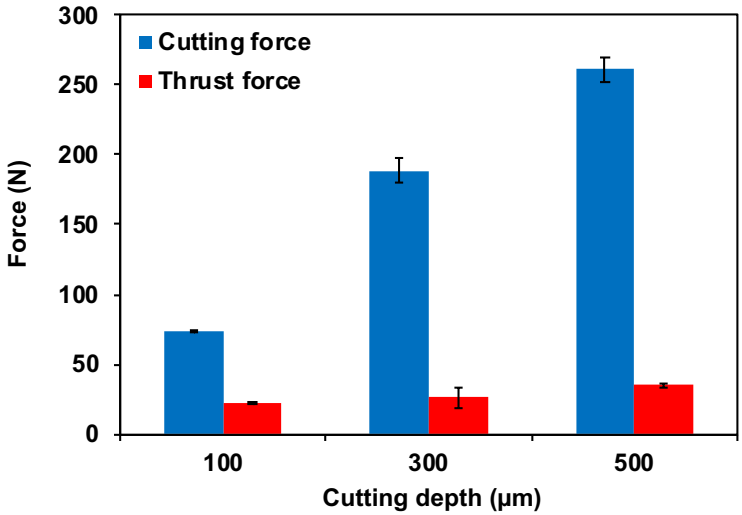

Figure 23: Machining forces of the orthogonal cutting process of UD flax FC with different values of cutting depth

4.5. Effect of sample temperature

The effect of NFC sample temperature on their machinability has been investigated on the same study of rake angle effect presented in section 4.3.3. The thermal investigation is performed by comparing the machining of NFC samples at room temperature (25ºC) and NFC samples that have been cooled up to 0ºC (directly before the tool passes across the sample) using a cooling spray (Chegdani et al., 2018b).

SEM images of Figure 24 show how lowering the sample temperature before machining influence the cutting behavior of flax fibers. At room sample temperature, flax fibers are deformed toward the cutting direction which makes their shearing difficult. Therefore, uncut fiber extremities are present on the machining surface in addition to some decohesion zones caused by interfaces damage (Figure 24(a)). This specific behavior of flax fiber was founded in many previous investigations in this chapter.

In the case of low sample temperature, cross sections of flax fibers seem to be smaller than that of fibers machined at room temperature (Figure 24(b)). This shows how much

flax fibers are deformed plastically during the cutting operation at room sample temperature. Flax fibers are much better sheared at low sample temperature which avoid the uncut fiber extremities and the high rate of decohesion zones. It can be concluded that lowering the sample temperature increases the cutting contact stiffness at fibers scale with enhances significantly their machinability.

Natural fiber composites considered in this study are manufactured with thermoplastic polymer of polypropylene. The choose of thermoplastic matrices are justified by their reversible transformation which gives to the NFC the ability to be recyclable. Moreover, natural fibers are composed of natural amorphous polymers (hemicellulose and lignin) at nanoscale. Consequently, the polymeric composition on NFC suggests that thermal conditions of machining could have an important impact on the machinability of NFC. Indeed, when decreasing the sample temperature, the rigidity of the polymeric components of the NFC increases and strengthen the fibers stiffness. This gives to the fibers the ability to resist to the transverse deformations caused by the tool crossing.

The thermal effect is also reproduced on the topographic response as shown in Figure 25. Lowering the sample temperature decreases the surface roughness by improving the shear efficiency of flax fibers in NFC.

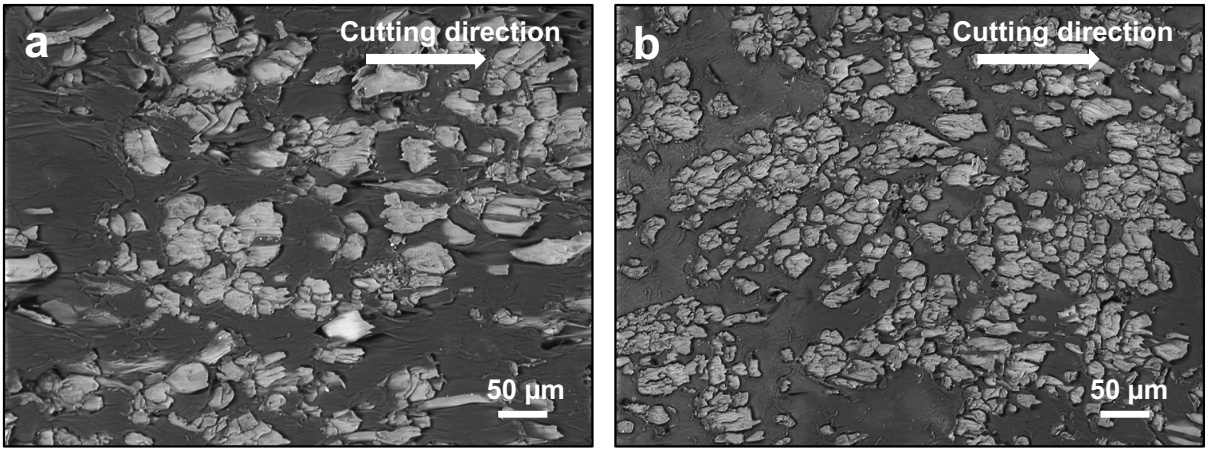

Figure 24: SEM images of the machined surfaces of UD flax FC at (a) room sample temperature and (b) low sample temperature

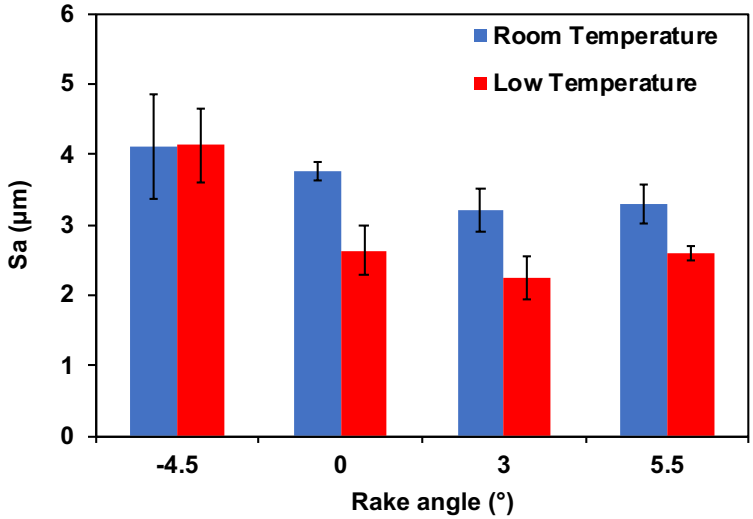

Figure 25: 3D arithmetic mean surface roughness of machined surfaces at room and low sample temperatures

5. Conclusions

Machining of natural fiber composites (NCF) performed with thermoplastic polymers has been investigated in this chapter. The machinability of NFC is analyzed regarding fibers properties, tool properties, and process parameters. A large exploratory study is presented to cover the main composite structures and the main industrial process applications. The following conclusions can be drawn:

- The removed chip remains continuous at large range of process parameters. This machining behavior of NFC is related to the its ductile behavior generated by the elastoplastic properties of both flax fibers and polymer matrix.
- The cutting behavior of natural fibers is dependent on their mechanical properties. The fiber shearing efficiency of increases by the fiber stiffness increase.
- A fiber orientation of 45º from the cutting direction offers the best fiber shearing and the best machinability of NFC.
- The machinability of NFC is highly dependent on tool geometry. This investigation concludes that the machining tools for NFC should have:

    - Small cutting edge radius which should be less than elementary fiber diameter;
    - Straight cutting flutes with zero helix angle;
    - Positive rake angle.
- Machining of NFC requires the use of:
    - A couple of cutting speed and feed speed that allows the generation of high feed rate: 0.14 – 0.16 mm/tooth is recommended in this study.
    - Small cutting depths to avoid fiber deformation and interfaces damage: 100 µm id recommended in this study.
- Lowering the sample temperature improves the machinability of NFC by increasing the cutting contact stiffness.

Nevertheless, the majority of these recommendations increases the cutting forces which can be harmful for cutting tools. Moreover, machining with low cutting edge radius means working with uncoated cutting tools which could increase significantly the tool wear. Therefore, deeper investigation should be performed to understand and optimize the wear of cutting tools when machining NFC.

6. References

Akampumuza, O., Wambua, P.M., Ahmed, A., Li, W., Qin, X.-H., 2017. Review of the applications of biocomposites in the automotive industry. Polym. Compos. 38, 2553–2569. https://doi.org/10.1002/pc.23847

Alves, C., Ferrao, P.M.C., Silva, A.J., Reis, L.G., Freitas, M., Rodrigues, L.B., Alves, D.E., 2010. Ecodesign of automotive components making use of natural jute fiber composites. J. Clean. Prod. 18, 313–327. https://doi.org/10.1016/J.JCLEPRO.2009.10.022

Baley, C., 2002. Analysis of the flax fibres tensile behaviour and analysis of the tensile stiffness increase. Compos. - Part A Appl. Sci. Manuf. 33, 939–948. https://doi.org/10.1016/S1359-835X(02)00040-4

Charlet, K., Baley, C., Morvan, C., Jernot, J.P., Gomina, M., Bréard, J., 2007. Characteristics of Hermès flax fibres as a function of their location in the stem and properties of the derived unidirectional composites. Compos. Part A Appl. Sci. Manuf. 38, 1912–1921. https://doi.org/10.1016/j.compositesa.2007.03.006

Chegdani, F., El Mansori, M., 2018. Friction scale effect in drilling natural fiber composites. Tribol. Int. 119, 622–630. https://doi.org/10.1016/j.triboint.2017.12.006

Chegdani, F., El Mansori, M., Mansori, M. El, El Mansori, M., 2018a. Mechanics of material removal when cutting natural fiber reinforced thermoplastic composites. Polym. Test. 67, 275–283. https://doi.org/10.1016/j.polymertesting.2018.03.016

Chegdani, F., Mezghani, S., El Mansori, M., 2016. On the multiscale tribological signatures of the tool helix angle in profile milling of woven flax fiber composites. Tribol. Int. 100, 132–140. https://doi.org/10.1016/j.triboint.2015.12.014

Chegdani, Faissal, Mezghani, S., El Mansori, M., 2015. Experimental study of coated tools effects in dry cutting of natural fiber reinforced plastics. Surf. Coatings Technol. 284, 264–272. https://doi.org/10.1016/j.surfcoat.2015.06.083

Chegdani, F, Mezghani, S., El Mansori, M., Mkaddem, A., 2015. Fiber type effect on tribological behavior when cutting natural fiber reinforced plastics. Wear 332–333, 772–779. https://doi.org/10.1016/j.wear.2014.12.039

Chegdani, F., Takabi, B., Tai, B.L., Mansori, M. El, Bukkapatnam, S.T.S., 2018b. Thermal Effects on Tribological Behavior in Machining Natural Fiber Composites. Procedia Manuf. 26, 305–316. https://doi.org/10.1016/J.PROMFG.2018.07.039

Davim, J.P., Reis, P., 2005. Damage and dimensional precision on milling carbon fiber-reinforced plastics using design experiments. J. Mater. Process. Technol. 160, 160–167. https://doi.org/10.1016/j.jmatprotec.2004.06.003

Dittenber, D.B., GangaRao, H.V.S., 2012. Critical review of recent publications on use of natural composites in infrastructure. Compos. Part A Appl. Sci. Manuf. https://doi.org/10.1016/j.compositesa.2011.11.019

Etaati, A., Mehdizadeh, S.A., Wang, H., Pather, S., 2014. Vibration damping characteristics of short hemp fibre thermoplastic composites. J. Reinf. Plast. Compos. 33, 330–341. https://doi.org/10.1177/0731684413512228

Khan, R.A., Sharmin, N., Khan, M.A., Das, A.K., Dey, K., Saha, S., Islam, T., Islam, R., Nigar, F., Sarker, B., Debnath, K.K., Saha, M., 2011. Comparative studies of mechanical and interfacial properties between jute fiber/PVC and e-glass fiber/PVC composites. Polym. - Plast. Technol. Eng. 50, 153–159. https://doi.org/10.1080/03602559.2010.531422

Morvan, C., Andème-Onzighi, C., Girault, R., Himmelsbach, D.S., Driouich, A., Akin, D.E., 2003. Building flax fibres: more than one brick in the walls. Plant Physiol. Biochem. 41, 935–944. https://doi.org/10.1016/j.plaphy.2003.07.001

Nassar, M.M.A., Arunachalam, R., Alzebdeh, K.I., 2017. Machinability of natural fiber reinforced composites: a review. Int. J. Adv. Manuf. Technol. 88, 2985–3004. https://doi.org/10.1007/s00170-016-9010-9

Pandey, J.K., Ahn, S.H., Lee, C.S., Mohanty, A.K., Misra, M., 2010. Recent Advances in the Application of Natural Fiber Based Composites. Macromol. Mater. Eng. 295, 975–989. https://doi.org/10.1002/mame.201000095

Pickering, K.L., Aruan Efendy, M.G., Le, T.M., 2016. A review of recent developments in natural fibre composites and their mechanical performance. Compos. Part A Appl. Sci. Manuf. 83, 98–112. https://doi.org/10.1016/J.COMPOSITESA.2015.08.038

Rajeshkumar, G., Hariharan, V., 2014. Free Vibration Characteristics of Phoenix Sp Fiber Reinforced Polymer Matrix Composite Beams. Procedia Eng. 97, 687–693. https://doi.org/10.1016/J.PROENG.2014.12.298

Ramesh, M., Palanikumar, K., Hemachandra Reddy, K., 2017. Plant fibre based bio-composites: Sustainable and renewable green materials. Renew. Sustain. Energy Rev. 79, 558–584. https://doi.org/10.1016/J.RSER.2017.05.094

Sadrmanesh, V., Chen, Y., 2019. Bast fibres: structure, processing, properties, and applications. Int. Mater. Rev. 64, 381–406. https://doi.org/10.1080/09506608.2018.1501171

Shalwan, A., Yousif, B.F., 2013. In State of Art: Mechanical and tribological behaviour of polymeric composites based on natural fibres. Mater. Des. 48, 14–

24. https://doi.org/10.1016/j.matdes.2012.07.014

Yu, C., 2015. Natural Textile Fibres: Vegetable Fibres, in: Textiles and Fashion: Materials, Design and Technology. Woodhead Publishing, pp. 29–56. https://doi.org/10.1016/B978-1-84569-931-4.00002-7

Zimniewska, M., Wladyka-Przybylak, M., Mankowski, J., 2011. Cellulosic Bast Fibers, Their Structure and Properties Suitable for Composite Applications, in: Cellulose Fibers: Bio- and Nano-Polymer Composites. Springer Berlin Heidelberg, Berlin, Heidelberg, pp. 97–119. https://doi.org/10.1007/978-3-642-17370-7_4